Inclusion study in zircon from ultrahigh-pressure metamorphic rocks in the Kokchetav massif: an excellent tracer of metamorphic history

Ikuo Katayama[1,*] and Shigenori Maruyama[2]

[1]*Department of Earth and Planetary Systems Science, Hiroshima University, Hiroshima 739-8526, Japan*

[2]*Department of Earth and Planetary Sciences, Tokyo Institute of Technology, Tokyo 152-8551, Japan*

*Corresponding author:

Department of Earth and Planetary Systems Science, Hiroshima University

Higashi-Hiroshima, Hiroshima 739-8526, Japan

Tel: +81-824-24-7468, Fax: +81-824-24-0735,

E-mail: katayama@hiroshima-u.ac.jp

Abstract

Zircon is an excellent capsule to preserve complex history of ultrahigh-pressure (UHP) metamorphic rocks, whereas mineralogical evidences of UHP conditions were mostly obliterated in the matrix assemblages due to extensive retrograde overprinting during exhumation. Zircons from the Kokchetav UHP-HP massif contain numerous inclusions of graphite, quartz, garnet, omphacite, jadeite, phengite, phlogopite, rutile, albite, K-feldspar, amphibole, zoisite, kyanite, calcite, dolomite, apatite and monazite, as well as the diagnostic UHP minerals, such as microdiamond and coesite, which were identified by laser Raman spectroscopy. Internal structure of zircon displays distinct zonation texture, which comprise inherited core, wide mantle and outer rim, each with distinctive inclusion micro-assemblages. The low-pressure mineral inclusions, such as graphite, quartz and albite, are common in the inherited core and thin outer rim, whereas diamond, coesite and jadeite occupy the mantle domain. The zircon core and outer rim is of detrital and relatively low-grade metamorphic origin, whereas the mantle domain is of HP to UHP metamorphic origin. Mineral assemblage and chemistry of inclusions preserved in zircon have used to constrain the metamorphic *P-T* path of the Kokchetav UHP-HP rocks, which results the peak metamorphism at 60-80 kbar and 970-1100^{o}C followed by nearly isothermal decompression at 10 kbar and ~800^{o}C. SHRIMP U-Pb spot analyses of the zoned zircon result four discrete ages of the Kokchetav metamorphic evolution; (1) Middle Proterozoic protolith age, (2) 537 ± 9 Ma for UHP metamorphism, (3) 507 ± 8 Ma for the late-stage amphibolite facies overprint, and (4) 456-461 Ma for post-orogenic thermal events. This indicates that Middle Proterozoic supracrustal protoliths of the Kokchetav UHP-HP rocks were subducted to mantle depths in

the Middle Cambrian, and exhumed to mid-crustal levels in the Late Cambrian. The zonal arrangement of inclusions and the presence of coesite and diamond without back reaction imply that aqueous fluids were low to absent within zircon, and is capable of retaining minerals of each metamorphic stage where Zr-saturated fluids are available. We suggest that inclusion study in zircon is a powerful method to clarify the multiple stages and timing of metamorphic evolution of the UHP-HP rocks, which elsewhere has been more or less obliterated in the host rock.

Introduction

The discovery of *in-situ* metamorphic microdiamonds in garnet biotite gneisses, dolomitic carbonates and garnet pyroxenites from the Kokchetav massif (Sobolev & Shatsky 1990) has greatly increased estimates of the maximum pressure attained by crustal metamorphic rocks in collisional orogenic belts. The tectonic and petrological implications for subduction of continental materials to depth in excess of 150 km has led to considerable interest in these unique rocks and their metamorphic evolution (e.g., Coleman & Wang 1995; Liou *et al*. 1994; Harley & Carswell 1995). However, vestiges of ultrahigh-pressure (UHP) metamorphic mineral assemblages constitute only a minor component of these rocks (e.g., Liou *et al*. 1994; Harley & Carswell 1995; Coleman & Wang 1995), which have been mostly obliterated by extensive hydration and replaced by low pressure mineral assemblages during a late amphibolite facies overprinting related to exhumation. Mineralogical evidence of the extreme conditions of UHP metamorphism is largely restricted to armored inclusions within refractory minerals such as garnet and zircon. Harley & Carswell (1995) considered that this problem is related to access of

fluids into the rocks undergoing metamorphism because of their catalytic role in promoting reactions (Rubie 1986; Austrheim 1998). Hence, zircon is considered to be the best container of UHP metamorphic minerals due to its wide *P-T* range stability and mechanical resistance, and is ubiquitous occurrence as an accessory mineral in metamorphic rocks (Chopin & Sobolev 1995; Tabata *et al*. 1998). We have systematically investigated mineral inclusions preserved in zircon from varying rocks in the Kokchetav massif to revel primary mineral assemblages and metamorphic zonation in this area. The distribution of micro-inclusions in zircon shows a good correlation with the zircon zonal texture, and we dated such zircon by SHRIMP U-Pb spot analysis to constrain the timing of discrete stages of metamorphic evolution. This paper summarize our recent progress on understanding the metamorphic *P-T*-time path of the Kokchetav UHP-HP rocks and we propose that micro-inclusion study preserved in zircon is a powerful tool to understand the complex metamorphic history of deeply subducted materials.

Geological outline of the Kokchetav UHP-HP massif

The Kokchetav massif is situated in the central domain of the composite Eurasian craton, and was formed during Cambrian collisional orogenic events (Dobretsov *et al.* 1995). This massif is composed of several Precambrian rock series, Cambro-Ordovician volcanic and sedimentary rocks, Devonian volcanic molasse, and Carboniferous-Triassic shallow-water and lacustrine sediments; these rocks were intruded by multi-stage granitoids (Dobretsov *et al.* 1995). The UHP-HP metamorphic part of the massif is a thin (1-2 km), more or less coherent, subhorizontal sheet, which is structurally overlain by a weakly metamorphosed unit (unit V), and underlain by the Daulet Suite (Kaneko *et al.* 2000). The UHP-HP massif is subdivided

into four units based on gross lithological variations (Fig. 1). Unit I is composed of amphibolite and acidic gneiss, unit II is composed mainly of pelitic-psammitic gneiss with locally abundant eclogite boudins and marble, unit III is composed of alternating of orthogneiss and amphibolite with rare eclogite lenses, and unit IV is composed of quartz schist and siliceous schist (Kaneko *et al.* 2000). Eclogites occur as lenticular masses within diamond-bearing gneiss and marble, and yield maximum *P-T* conditions of $P > 60$ kbar and $T > 1000$°C based on the K_2O-in-augite geobarometer and Grt-Cpx geothermometer (Okamoto *et al.* 2000). Metamorphic diamonds have been identified in pelitic gneisses, marbles and garnet pyroxenites from the Kumdykol region (Sobolev & Shatsky 1990; Zhang *et al.* 1997; Ogasawara *et al.* 2000; Katayama *et al.* 2000a), which is located in the central part of the massif (Fig. 1). Coesite also widely occurs in eclogite, pelitic gneiss and whiteschist as inclusions in zircon and garnet from the Kumdykol, Barchikol and Kulet (Shatsky *et al.* 1995; Korsakov *et al.* 1998; Parkinson 2000; Katayama *et al.* 2000a). Other mineralogical and textural indicators of UHP metamorphism, such as exsolved silica rods in omphacite, K-rich pyroxene, Si-rich phengite, and aluminous titanite are also present in the Kokchetav UHP-HP part of the massif (Shatsky *et al.* 1995; Zhang *et al.* 1997; Okamoto *et al.* 2000; Ogasawara *et al.* 2000, 2002; Katayama *et al.* 2000b).

Previous geochronological studies have reported the timing of the Kokchetav UHP-HP metamorphism using various methods. A mean U-Pb zircon age from diamond-bearing gneisses of 530 ± 7 Ma was interpreted to represent the peak-metamorphic age (Claoue-Long *et al.* 1991). Zircon xenocrysts as old as 2000 Ma have also been reported as Early Proterozoic protolith age (Claoue-Long *et al.* 1991). Clinopyroxene and garnet from eclogite

were dated at 533 ± 20 Ma by Sm-Nd isochron method (Jagoutz *et al.* 1990). Muscovite and biotite separated from diamond-bearing gneiss yielded ^{40}Ar-^{39}Ar ages of 517 ± 5 Ma and 516 ± 5 Ma, respectively, which have been interpreted as a cooling age (Shatsky *et al.* 1999).

Primary assemblages of ultrahigh-pressure conditions

Mineral inclusions in zircon from the Kokchetav UHP-HP rocks

We analyzed total ~12000 zircon separated from 246 representative rock samples from each metamorphic zone of the Kokchetav UHP-HP massif, including para- and ortho gneisses/schists, eclogites, marbles and quartz schist. After crushing and sieving of approximately 200 g of sample, and magnetic and heavy liquid separation of minerals, 50 to 500 zircon grains of approximately 100 μm diameters were hand-picked from the residue. Approximately half of the samples proved to be barren at this stage. The zircon grains (total approximately 12000 grains) were then mounted in epoxy and polished. Discrete inclusions in zircons were identified using laser Raman spectroscopy with the 514.5 nm line of an Ar laser.

Abundant microdiamond inclusions in zircon were identified in pelitic gneisses and dolomitic marbles from the Kumdykol region, which located in the central portion of this massif. The diamond-bearing zircons were usually rounded and colorless with 100-150 μm in size. In the host rocks, primary minerals were mostly replaced by amphibolite facies mineral assemblages such as chlorite, amphibole and plagioclase. Diamond inclusions in zircon were confirmed by the characteristic Raman peak at 1333 ± 2 cm^{-1} (Fig. 3a). Morphological forms comprise both octahedral and polycrystalline aggregates, approximately 10 μm in diameter. Other UHP-HP inclusions such as coesite, jadeite and garnet coexist with diamond inclusion

in zircon (Fig. 2). In addition, low-P minerals, including graphite, quartz and plagioclase were also recognized as inclusion in zircon separated from the same sample. Graphite occurs as intergrowths with microdiamonds that display a botryoidal habit, and clearly grew at the expense of graphite (Fig. 2f), whereas diamonds found in garnet are commonly surrounded by graphite along cracks, due to ingress of fluids. Coarse-grained graphite occurs in zircon core, although most diamonds distributed within mantle domain, and occasionally, small amounts of graphite also occur in the zircon outer rim. The inclusion micro-assemblages show a good correlation with the host zircon zonal texture seen in back-scattered electron (BSE) and cathodoluminescence (CL) images as described in later section.

Coesite inclusions are identified in zircon separated from diamond-bearing pelitic gneisses, marbles, and eclogites from Kumdykol, and quartz schist from Barchikol. Zircons from eclogites are subhedral to anhedral, and generally homogeneous in BSE image. Grain sizes were relatively smaller (50-80 μm) than those in diamond-bearing gneisses. Most coesite inclusions in zircon are ovoid, and up to 10 μm in diameter (Fig. 2), which are identified by the characteristic Raman spectrum at 523 ± 2 cm^{-1} and weaker peaks at 271 ± 1 cm^{-1}, 181 ± 2 cm^{-1} and 149 ± 1 cm^{-1} (Fig. 3b). Diamond-bearing dolomitic marble also contains coesite as inclusion in zircon, whereas SiO_2 phases were absent in matrix assemblages. This suggests that silica phases were completely consumed by the prograde reaction; dolomite + SiO_2 = diopside + CO_2, whereas zircon preserved relict coesite as inclusion.

Zircons separated from the other regions contain relatively low-*P* mineral inclusions, and show different characteristics compared to the UHP phase-bearing zircons; they are

euhedral, elongated and prismatic, and usually exhibit oscillatory zonal fabrics. Apatite and quartz inclusions are ubiquitous in these zircons, and rutile and phengite inclusions are commonly observed (Table 1).

Inclusion assemblages preserved in zircon and metamorphic facies

Primary UHP metamorphic minerals are more or less obliterated during pervasive retrograde metamorphism, especially in country gneisses due to ingress of fluids into the host rocks. The fragmental, incomplete evidence of UHP metamorphism provided by matrix assemblages greatly obscures characterization of metamorphic zonation in UHP metamorphic terranes. Attempts to constrain the metamorphic zonation in the Kokchetav massif were performed on the basis of mineral assemblages in metabasites (Ota *et al.* 2000; Masago 2000). The metabasites were divided into three metamorphic zones: (i) epidote-amphibolite facies, (ii) amphibolite facies, and (iii) eclogite facies. However, thus far, the matrix mineral assemblages in metabasites cannot further subdivide eclogite facies rocks because of the lack of UHP minerals in matrix assemblages due to the extensive overprinting. Our results of zircon-hosted inclusion distribution in this massif can be used to further subdivide the eclogite-facies rocks, including both metabasites and country gneisses, into diamond-eclogite, coesite-eclogite, and quartz-eclogite zones, whereas mineral assemblages in the matrix contain little evidence of such UHP assemblages (Fig. 4). Although coesites were reported in garnet from the Kulet region (Parkinson 2000), the lack of UHP evidences in zircon from this region can be due to low Zr contents in the bulk rocks and no further zircon growth in these rocks. However, zircon is generally ubiquitous in metamorphic rocks, and can protect primary

UHP minerals from late-stage overprinting. The metamorphic facies of UHP rocks can therefore be classified not only from matrix mineral assemblages but also from mineral inclusions in zircon. The identification of UHP mineral inclusions in zircon is now widely reported from other UHP metamorphic terranes including Dora-Maira massif of the western Alps (Schertle & Schreyer 1996), Western Gneiss Region in Norway (Carswell *et al.* 2001), Erzgebirge in Germany (Massonne 2001), Dabie Mountains (Tabata *et al.* 1998; Liu *et al.* 2001) and Sulu region (Ye *et al.* 1999; Liu *et al.* 2002), north Qaidam in northwest China (Song *et al.* 2001), Sulawesi in Indonesia (Parkinson & Katayama 1999), Kaghan valley in the Pakistan Himalaya (Kaneko *et al.* 2003) and southeast Brazil (Parkinson *et al.* 2001).

Mineral compositions of inclusions in zircon

Clinopyroxenes in both eclogite and marble exhibit exsolution texture of quartz and phengite (Fig. 5a,b). Other exsolution textures are also commonly observed in UHP metamorphic rocks, including ilmenite rods in olivine and clinopyroxene, magnetite plates or rods in olivine and clinohumite, monazite lamellae in apatite, and clinopyroxene needles in garnet (see compilation of Liou *et al.* 1998). Such exsolution textures are believed to form during decompression stage (Liou *et al.* 1998), however what mechanism produces the exsolution texture is not clear. Mineral inclusion preserved in zircon can preserve pre-exsolved chemical compositions and have constraint on the exsolution mechanism of the UHP phases.

Clinopyroxene

Abundant quartz rods occur in matrix omphacite of eclogite from Kumdykol (Fig. 5a), whereas zircon-hosted omphacite inclusions have no exsolution lamellae (Fig. 5c,d). Omphacite inclusions in zircon have significant amounts (up to 9.6 mol%) of the Ca-Eskola component ($Ca_{0.5}\square_{0.5}AlSi_2O_6$, where $\square$ is a vacancy on the M_2 site), in contrast to the small amounts (1.3 mol%, on average) in the matrix omphacite. We calculated the original composition of matrix omphacite based on the quartz exsolution volume. The results indicate 6.6 mol% Ca-Eskola component in the original omphacite, which agree with the inclusion composition in zircon. Figure 6 shows omphacite compositions plotted on a ternary Augite–Jadeite–Ca-Eskola diagram. Zircon-hosted omphacite tends to have higher Ca-Eskola component than matrix omphacite. The significant differences in the Ca-Eskola component between inclusion and matrix omphacite indicate that the quartz exsolution in matrix omphacite can be produced by a breakdown of this component. We therefore suggest that the Ca-Eskola component, which included at peak metamorphic conditions, broke down by the following reaction:

$$2\ Ca_{0.5}\square_{0.5}AlSi_2O_6 = CaAl_2SiO_6 + 3\ SiO_2 \qquad (1)$$

resulting in the exsolution of quartz rods in matrix omphacite. The vacancy-containing Ca-Eskola clinopyroxene is reported to be sensitive to pressure and highly unstable at lower pressures (Mao 1971; Smyth 1980). Recent experimental studies found, in addition to pressure, Ca-Eskola component is also sensitive to temperature and bulk composition (Konzett *et al*. 2008).

Rare jadeitic clinopyroxene inclusions were identified in the diamond-bearing biotite gneiss, whereas such clinopyroxenes are absent in the matrix phase. The jadeite inclusions also contain high Ca-Eskola component (13.4-18.6 mol%, Fig. 6). The higher Ca-Eskola component compared to those from eclogite may result from a high Al bulk composition.

Diopside in a diamond-bearing dolomitic marble contains abundant exsolved lamellae, which are a few μm in diameter and approximately 10 μm in length (Fig. 5b). It was difficult to obtain an accurate composition of the exsolution lamellae, however elemental mapping shows Al and K concentrations in the lamellae, and laser Raman spectroscopy exhibits typical spectra of phengite with 260 cm^{-1} and 702 cm^{-1} peaks. The exsolution textures are, however, absent in the inclusion in zircon (Fig. 5e), and inclusions contain significant high K_2O and Ca-Eskola components, up to 0.56 wt% and 3.5 mol% respectively, although matrix diopside contains much less K_2O content (0.14 wt%) and CaEs component (2.1 mol%). Recalculated composition of matrix diopside involving 2.16 wt% phengite lamellae indicates 0.4 wt% K_2O and 2.7 mol% Ca-Eskola components for the original diopside, which is mostly consistent with compositions of the diopside inclusions in zircon. These suggest a following reaction to produce the phengite exsolution in diopside:

$$6\ KAlSi_2O_6 + 4\ Ca_{0.5}\square_{0.5}AlSi_2O_6 + 3\ (Mg,Fe)_2Si_2O_6 + CaAl_2SiO_6 + 6\ H_2O$$
$$= 3\ Ca(Mg,Fe)Si_2O_6 + 6\ K(Mg,Fe)_{0.5}Al_2Si_{3.5}O_{10}(OH)_2$$

6 K-Jd + 4 CaEs + 3 Opx + CaTs + 6 water = 3 Aug + 6 Phn (2)

During decompression, K-jadeite and Ca-Eskola components become unstable at low

pressures and temperatures, and reaction (2) was promoted resulting the exsolution of phengite needles in matrix clinopyroxene. The phengite exsolution in diopside suggests that water included in phengite may have been initially incorporated within the precursor clinopyroxene at high pressures. According to the volume of phengite exsolution (2.6 volume%), the precursor diopside contains approximately 1000 ppm H_2O. Infrared and SIMS analyses reveal high water concentrations in clinopyroxene from eclogites, up to 1500 ppm H_2O (Katayama & Nakashima 2003; Katayama *et al.* 2006).

Garnet

Garnet inclusions in zircon from the coesite-bearing eclogite are rare compared to omphacite inclusion. Chemical composition of garnets from both inclusion and matrix is plotted on the ternary diagram of (Alm+Sps)-Prp-Grs (Fig. 7). Matrix garnets have almost homogeneous composition, slightly zoned with decreasing pyrope content from core to rim. On the other hand, garnet inclusions show a wide compositional variation, four crystals are Alm-rich (47-53%) and contain considerable spessartine (0.9-1.2%) component whereas the other grains are consistent with matrix garnet. Garnets contain detectable Na_2O (up to 0.15 wt%), which is consistent with previous studies in this region (Shatsky *et al.* 1995; *Zhang et al.* 1997; Okamoto *et al.* 2000). The high sodium content in garnet coexisting with a Na-bearing mineral is considered to be one of the important indicators of UHP metamorphism as well as high K_2O content in clinopyroxene.

Abundant garnet inclusions were identified in zircon from the diamond-bearing pelitic gneiss. Garnet inclusions are clear single crystal and approximately 10 μm in diameter,

whereas matrix garnets are mostly fractured and replaced by secondary chlorite and biotite. Matrix garnet exhibits significant retrograde zonation with decreasing Prp contents from homogeneous core (24-26%) to rim (19-25%). Garnet inclusions show a relatively wide compositional range, extending toward the pyrope end-member. The maximum Prp content in garnet inclusions (29 mol%) is slightly higher than those in matrix (26 mol%). Garnet in the diamond-bearing gneiss also contains significant amounts of sodium, up to 0.19 wt% Na_2O.

Rare garnet inclusions were identified in zircon from the diamond-bearing marble. They coexist with diamond inclusions in same zircon grain, and have high Grs (44%) and Prp (33%) components, whereas garnet is absent in matrix assemblage. Although garnets contain relatively high amounts of Na_2O content from other lithologies in Kumdykol, sodium content is negligible in garnet from the diamond-bearing marble.

Micas

Phengite inclusions in zircon show higher Si content than those in matrix phengite from pelitic gneisses (up to 3.57 per 11 oxygens, Fig. 8), whereas Fe/(Fe+Mg) ration of inclusion and matrix phengites is limited in each sample. Phengite inclusions in the diamond-bearing marble contain high Si (up to 3.53 per formula unit) with a very low Fe/(Fe+Mg) ratio of 0.06, although phengite is absent in zircon separated from the diamond-bearing gneiss and the coesite-bearing eclogite. Phlogopite inclusions coexisting microdiamond in zircon from marble contain higher Si content, 2.99-3.00 per 11 oxygens, and slightly higher Fe/(Fe+Mg) ratio of 0.11 than those of matrix phlogopite (2.28-2.92 Si value and 0.08-0.10 Fe/(Fe+Mg) ratio). The Al/(Al+Si) ratio of inclusion phlogopite is higher than that of matrix.

Zircon geochronology assisted by inclusion micro-assemblages

The Kokchetav UHP-HP rocks have experienced a long and complex metamorphic evolution over a very wide range of *P-T* conditions. Radiometric age dating is a key to understand the complex metamorphic history of the UHP-HP rocks. Sensitive high resolution ion micro-probe (SHRIMP) dating of discrete domains within zircon crystals, allied with cathodoluminescence (CL) image analysis, has contributed greatly to recent progress in dating metamorphic rocks (e.g., Gebauer *et al.* 1997; Rubatto *et al.* 1999; Liati & Gebauer 1999). Discrete zoned domains in zircon may reflect not only the peak-metamorphic stage, but also progressive and retrogressive stages of their metamorphic evolutions. This can be clarified by identification of mineral inclusion micro-assemblages within each zircon domain.

Internal structure of zircon associated with inclusions

Zircons from the diamond-bearing gneisses are usually rounded, colorless and 100-200 μm in diameter. The CL and BS investigations reveal internal structures of zircons, mainly consisting of core and rim domains; cores of low luminescence in CL image are surrounded by relatively bright luminescent rims (Fig. 9a,b). Complex zoned metamict cores rarely survive, and have relatively small domains of a bright luminescence in CL (Fig. 9a); they are interpreted as inherited domains. Zircons contain abundant microdiamond inclusions, and other include coesite, garnet, jadeitic pyroxene, rutile, phengite, kyanite, amphibole, plagioclase, chlorite, apatite, graphite and quartz (Table 1). Mineral inclusions are generally correlated with specific domains of zoned zircon. The core to mantle domains contain

diamond, coesite and jadeite inclusions, whereas graphite, quartz, plagioclase and chlorite inclusions occur in the outer rims, and most inherited cores are inclusion-free or contain low-*P* minerals such as graphite and quartz (Fig. 10).

A low-grade pelitic schist from the Sulu-Tjube region contains euhedral and elongated zircons of approximately 100 μm long axis length. The morphology of zircons is quite different from that in the diamond-bearing gneisses. In BS and CL images, zircons consist of small cores, widely spaced euhedral oscillatory domains as typically observed for crystal growth from a melt, and thin outer unzoned rims with BS-bright luminescence (Fig. 9c). The inner boundary of oscillatory domains and rims is irregular, in which the magmatic core is corroded by the homogeneous rims. These zircons contain quartz, muscovite, K-feldspar, chlorite, graphite and apatite as inclusion.

Eclogite contains abundant anhedral zircons of 50-70 μm in diameter, which is apparently smaller than those of the pelitic gneisses. Zircon separated from eclogite contains the UHP phases such as coesite, K-rich omphacite and Na-rich garnet, and also includes composite inclusion of garnet and albite (Okamoto *et al.* 2006). CL image reveals that most zircons are homogeneous without magmatic core (Fig. 9d).

Zircon SHRIMP U-Pb dating

U-Pb isotopic data of the diamond-bearing zircon domains are mostly concordant (Fig. 11), and yield apparent $^{206}Pb/^{238}U$ ages ranging from 554 to 493 Ma. They contain the UHP mineral inclusions, such as diamond and coesite, which clearly indicate the zircons have grown under UHP conditions. The zircon outer rims generally exhibit younger ages than those

of diamond-bearing cores, ranging from 456 to 517 Ma (Fig. 11). The considerable difference in the apparent ages occurs even in single zircon grains. The inherited core yields a discordant age (Fig. 11), indicating that it has been affected by one or more Pb-loss events. Assuming that Pb-loss from the core had occurred at the time of the latest metamorphism (ca. 500 Ma), the upper intercepts of presumed mixing lines (discordias) indicate that the core had grown or metamorphosed in the Middle Proterozoic (ca. 1300-1400 Ma). Zircons from low-grade schist yield $^{206}Pb/^{238}U$ ages of 1280-1140 Ma in the core and mantle domains, and apparently younger ages of 461-516 Ma in the outer rim (Fig. 12). The homogeneous zircons from the coesite-bearing eclogite are mostly concordant, and yield $^{206}Pb/^{238}U$ ages ranging from 569 to 506 Ma (Fig. 12). The large age variety and uncertainty may result from extremely low U concentration (42-66 ppm) in these zircon grains, whereas coesite and high Ca-Eskola omphacite inclusions clearly indicate that these zircons have grown at the UHP stages.

Zircon REE abundances

Rare earth element (REE) pattern and abundance of zircon are mostly similar between the diamond-bearing gneisses and eclogite, but significantly different in the low-grade schist (Fig. 13). In the diamond-grade gneisses, the inherited core show different pattern from those of metamorphic overgrowth and display relatively high heavy REE concentration and flat pattern, whereas the diamond-bearing UHP domains are characterized by steep pattern. The low-*P* mineral bearing rims show mostly same pattern of the UHP domains, but some have negative Eu anomaly. Zircons from eclogite have no Eu anomaly and exhibit mostly same pattern with those of the diamond-grade UHP domains. In the low-grade schist, zircon show clearly

different REE pattern, characterized by higher abundance of light REE and significant negative Eu anomaly. The metamorphic overgrowth shows slightly higher heavy REE concentration than those of the inherited core.

P-T-time history of the Kokchetav UHP-HP rocks

The ages obtained from SHRIMP analyses of different zircon domains suggest four discrete stages of the Kokchetav zircon growth: Middle Proterozoic for inherited cores, 537 ± 9 Ma for cores, 507 ± 8 Ma for rims, and 456-461 Ma for outer rims (Fig. 13). The core and rim ages are weighted mean ages with 2 sigma errors calculated using isoplot (Ludwig 1991), for which uncertainties are 95% confidence level.

An inherited zircon core of diamond-bearing gneiss yields a Middle Proterozoic age as an upper intercept age. The zircon core from low-grade schist yields a concordant age of 1280 ± 51 Ma, and oscillatory mantles yielded 1138-1143 Ma. This indicates the protolith of the Kokchetav UHP-HP rocks formed or was originally metamorphosed in the Middle Proterozoic. Claoue-Long *et al.* (1991) reported that zircon xenocrysts have concordant ages in the Early Proterozoic (ca. 2000 Ma). Protolith of the Kokchetav UHP-HP rocks therefore contain various components of Proterozoic age.

The 537 Ma age of the diamond-bearing domains is clearly related to the UHP (peak) metamorphism. This age is slightly older than that reported by Claoue-Long *et al.* (1991) of 530 ± 7 Ma. The discrepancy may be due to their calculation of the mean age involving various zircon domains including the UHP and later overprinting stages. Although the texture and distribution of inclusions suggest that some zircons have grown during prograde

metamorphism (Katayama *et al.* 2000a), the averaging of the UHP zircon domains may have prevented clearly differentiation between the ages of prograde and peak metamorphism. Various *P-T* conditions of the Kokchetav UHP-peak metamorphism have been estimated and summarized in Table 4 and Figure 14. The minimum peak pressure of 40 kbar at 800°C is constrained by the occurrence of microdiamonds. The high K_2O content in clinopyroxene (up to 1.0 wt%) from eclogite indicates a pressure over 60 kbar (Okamoto *et al.* 2000). Ogasawara *et al.* (2000) noted that the occurrence of dolomite in diamond-bearing dolomite marble constrains the maximum pressure over 70 kbar. Peak temperatures have been estimated using the garnet-clinopyroxene geothermometer, which yield 880-910°C (Zhang *et al.* 1997) from garnet-biotite gneiss, 950-1050°C (Okamoto *et al.* 2000), 920-1000°C (Shatsky *et al.* 1995) and 785°C (Zhang *et al.* 1997) from eclogite, and 960°C (Zhang *et al.* 1997) and 980°C (Ogasawara *et al.* 2000) from diamond-bearing dolomitic marble. The garnet-biotite and garnet-phengite geothermometers yield temperatures ranging from 800 to 920°C for garnet-biotite gneiss (Shatsky *et al.* 1995). In this study, garnet and clinopyroxene inclusions occur together in the zircon cores from the diamond-bearing gneiss. The Fe-Mg partitioning between garnet and clinopyroxene of Krogh (1988) yields peak temperatures of 920-1020°C at a pressure of 60 kbar. The calculated temperatures are mostly consistent with previous estimates of the UHP rocks, but are slightly higher than those of the garnet-biotite gneiss. This may result from the strong retrogression of matrix phases, whereas the inclusions in zircon have better preserved primary compositions of the UHP metamorphism. The 507 Ma age of the outer rims corresponds to late-stage metamorphic overprinting, because these domains surround diamond- and coesite-bearing cores, and contain low-*P* mineral inclusions

such as graphite, quartz, plagioclase and chlorite. Replacement of garnet by biotite, amphibole and/or plagioclase, and symplectite of plagioclase and amphibole after pyroxene in eclogite and pelitic gneiss, indicate that these rocks suffered amphibolite facies retrogression (Shatsky *et al*. 1995; Zhang *et al.* 1997; Okamoto *et al.* 2000). Ar/Ar ages of secondary muscovite and biotite have been reported to be 517 ± 5 Ma (Shatsky *et al*. 1999). They are slightly older than those of zircon rims, however, the Ar/Ar age and our zircon rim U/Pb age are within uncertainty. The variation of rim ages (488-517 Ma; Fig. 12) may reflect continuous retrogression from amphibolite facies to greenschist facies during exhumation. Zhang *et al*. (1997) estimated the retrograde temperatures of 680-790°C from recrystallization of garnet-biotite in marble and amphibole-plagioclase in eclogite at amphibolite facies condition. Symplectic intergrowth of ilmenite, albite, augite and amphibole between omphacite and garnet from eclogite indicates pressures lower than 10 kbar and temperatures ranging from 750 to 950°C (Zhang *et al*. 1997). In dolomitic marble, the highest $MgCO_3$ in Mg-calcite constrains the minimum *P-T* conditions higher than 25 kbar and 800°C for the exhumation stage (Ogasawara *et al.* 2000). Zircon from the diamond-bearing gneiss contains chlorite inclusions of similar composition to those of matrix chlorite. Matrix garnets are replaced by chlorite, and the Fe-Mg partitioning geothermometer between garnet and chlorite (Grambling 1990) yields temperatures of 740-790°C at pressure of 10 kbar (Fig. 14). In low-grade schist of the Daulet Suite, zircons showed no age component around 537 Ma, and outer zircon rims yield 461-516 Ma, which are similar to the retrograde ages of the diamond-bearing gneisses. The low-grade rocks have been experienced maximum *P-T* conditions of ~2.5 kbar and 500-650°C (Terabayashi *et al.* 2002). Two outer rim domains yield apparently younger ages

of 456-460 Ma (Fig. 12). They are interpreted to originate from late thermal events related to the large volume of granitoids intrusions in the Ordovician-Silurian (Dobretsov *et al.* 1995).

Tectonic implications

These data indicates that Middle Proterozoic supracrustal rocks were subducted with downgoing oceanic lithosphere to mantle depths during Middle Cambrian times (527-554 Ma). The ultrahigh pressure metamorphism took place at depths exceeding 150 km where microdiamond and coesite were crystallized and trapped in zircon during this stage. The deeply subducted supracrustal rocks have been returned to mid-crustal levels in the Late Cambrian (488-517 Ma).

Various exhumation mechanisms of UHP metamorphic rocks from mantle depths have been proposed (e.g., Ernst 1971; Hacker &Peacock 1995; Maruyama *et al.* 1996). Taking the weighted mean ages of UHP metamorphism (537 ± 9 Ma) and late amphibolite facies overprinting (507 ± 8 Ma), exhumation from diamond-grade depths (ca. 60 kbar, 1000°C) to mid-crustal depths (ca. 10 kbar, 800°C) must have been completed within about 30 Ma (Fig. 14). This suggests that about 150 km of uplift must have occurred within about 30 My, leading to an average exhumation rate of 5 km/My. However, this is minimum rate because the mean ages of zircon cores and rims may include the prograde metamorphism and the later greenschist facies overprinting, respectively. Considering extreme error values of the core and rim ages, the maximum exhumation rate is estimated to be about 12 km/My. Although Hermann *et al.* (2001) reported indistinguishable ages between UHP and retrograde zircon domains and gave a significant fast exhumation rate of ~20 km/My, our detail analyses of

mineral inclusions preserved in zircon show clearly distinct ages of different zircon domains. The exhumation rate estimated here lies in the same range as those calculated for the Dora Maira massif of Western Alps (Gebauer *et al.* 1997), the Betic Cordilleras of northern Spain (Zeck & Whitehouse 1999), the central Rhodope zone of northern Greece (Liati & Gebauer 1999), and for the Dabie Mountains of central China (Maruyama *et al.* 1998). The relatively rapid exhumation is considered to be one of the factors for preservation of UHP mineral assemblages and prograde zonation of garnet in whiteschist (Parkinson 2000), which would be obliterated by a long time span at high temperatures and pressures. The rapid exhumation rate suggests slab decoupling between continental and oceanic lithospheres, resulting in isostatic rebound of sialic material, as a most plausible driving force for uplift of the Kokchetav UHP metamorphic rocks from mantle depths. This is consistent with geological and petrological evidences in the Kokchetav massif; subhorizontal internal structural fabrics and metamorphic zonation, paired subhorizontal bounding structures juxtaposing the nappe against lower grade or unmetamorphosed rock (Kaneko *et al.* 2000), the thermobaric structure with the highest-grade (UHP) rocks occupying a medial position within the nappe (Ota *et al.* 2000). The exhumed UHP rocks were juxtaposed against lower grade rocks of the Daulet Suite in the Late Cambrian. The tectonic juxtaposition of the dehydrated UHP-HP rocks underlying the low-grade Daulet Suite rocks would allow infiltration of fluids and effectively obliterate the UHP-HP matrix mineral assemblages. In Ordovician to Silurian times (< 461 Ma), the post-orogenic granitic rocks intruded and were contemporaneous with widespread secondary normal faulting in the Kokchetav UHP-HP massif.

Conclusions

(1) UHP mineral inclusions, including diamond and coesite, were preserved in zircon from the Kokchetav UHP-HP massif, whereas those UHP evidences were mostly obliterated in the matrix assemblages due to the extensive overprinting during exhumation. In addition to the UHP phases, relicts of prograde texture including diamond crystallization consuming graphite are identified as inclusion in zircon. The preservation of primary UHP and prograde evidences in zircon is most likely due to impervious to fluid infiltration and zircon is capable of retaining minerals of each metamorphic stage.

(2) Mineral inclusions exhibit a slightly different chemical composition compared to the matrix minerals. Clinopyroxene inclusions from eclogite contain higher Ca-Eskola component, up to 9.6 mol%, than those of matrix, and the breakdown of this component causes quartz exsolution in the matrix clinopyroxenes. Mineral compositions of inclusion preserved in zircon can constrain the metamorphic *P-T* conditions, which results the peak stage of 60-80 kbar and 900-1100°C, 740-790°C and about 10 kbar for the retrograde stage.

(3) SHRIMP U-Pb dating of zircons assisted by inclusion micro-assemblages results four discrete timing of the Kokchetav UHP metamorphic evolution: Middle Proterozoic protolith age, 537 ± 9 Ma for the UHP metamorphism, 507 ± 8 Ma for the late-stage amphibolite facies overprint, and 456-461 Ma for post-orogenic thermal events. Although previous geochronological studies used different isotopic systems to constrain the metamorphic evolution, zircon geochronology assisted by inclusion micro-assemblages enable to provide discrete timing of each stage of the complex metamorphic history of the UHP-HP rocks.

Acknowledgments

We thank C.D. Parkinson, Y. Kaneko, T. Ota, S. Omori, K. Okamoto, Y. Ogasawara, R.Y. Zhang, K. Ye, F. Liu and M. Ohta for discussion and suggestion, and H. Tabata, K. Yamauchi, N. Abe, T. Iizuka, Y. Sano, K. Terada, and Y. Tsutsumi for various analytical assistances. A. Zayachikovsky is gratefully acknowledged for helping separation of large number of zircon. This study was supported by the Japan Society for the Promotion of Science.

References

ANDERS, W. & GREVESSE, N. 1989. Abundances of the elements: Meteoritic and solar. *Geochimica et Cosmochimica Acta*, **53**, 197-214.

AUSTRHEIM, H. 1998. Influence of fluid and deformation on metamorphism of deep crust and consequences for the geodynamics of collision zones. *In:* HACKER, B.R. & LIOU, J.G. (eds) *When Continents Collide: Geodynamics and Geochemistry of Ultrahigh-Pressure Rocks.* Kluwer Academic Publishers, 297-323.

BOHLEN, S.R. & BOETTCHER, A.L. 1982. The quartz-coesite transformation: A pressure determination and effects of other components. *Journal of Geophysical Research*, **87**, 7073-7078.

BUNDY, F.P. 1980. The P, T phase and reaction diagram for elemental carbon, *Journal of Geophysical Research*, **85**, 6930-6936.

CARSWELL, D.A., BRUECKNER, H.K., CUTHBERT, S.J., KROGH, T.E., MEHTA, K., O'BRIEN, P.J. & TUCKER, R.D. 2001. Coesite preservation within zircons in the Hareidland eclogites and the timing of ultrahigh-pressure metamorphism in the Western Gneiss Region of Norway. *In: Fluid/slab/mantle interactions and ultrahigh-P minerals: UHPM Workshop* (extended abstract), Waseda University, Tokyo, 111-115.

CHOPIN, C. AND SOBOLEV, N.V., 1995. Principal mineralogic indicators of UHP in crustal rocks. *In:* COLEMAN R.G. & WANG X. (eds) *Ultrahigh-pressure Metamorphism*, Cambridge University Press, 96-133.

CLAOUE-LONG, J.C., SOBOLEV, N.V., SHATSKY, V.S & SOBOLEV, A.V. 1991. Zircon response to diamond pressure metamorphism in the Kokchetav massif, USSR. *Geology*, **19**, 710-713.

COLEMAN, R. G. & WANG, X., 1995. Overview of the geology and tectonics of UHPM. *In:* COLEMAN R.G. & WANG X. (eds) *Ultrahigh-pressure Metamorphism*, Cambridge

University Press, 1-28.

DOBRETSOV, N.L., SOBOLEV, N.V., SHATSKY, V.S., COLEMAN, R.G. & ERNST, W.G. 1995. Geotectonic evolution of diamondiferous paragneisses, Kokchetav complex, northern Kazakhstan - the geologic enigma of ultra-high pressure crustal rocks within a Palaeozoic foldbelt. *The Island Arc*, **4**, 267-279.

ERNST, W.G. 1971. Metamorphic zonations on presumably subducted lithospheric plates from Japan, California, and the Alps. *Contribution to Mineralogy and Petrology*, **34**, 45-59.

GEBAUER, D., SCHERTL, H.P., BRIX, M. & SCHREYER, W. 1997. 35 Ma old ultrahigh-pressure metamorphism and evidence for very rapid exhumation in the Dora Maira Massif, Western Alps. *Lithos*, **41**, 5-24.

GRAMBLING, J.A. 1990. Internally-consistent geobarometry and H_2O barometry in metamorphic rocks: the example garnet-chlorite-quartz. *Contribution to Mineralogy and Petrology*, **105**, 617-628.

HACKER, B.R. & PEACOCK, S.M. 1995. Creation, preservation and exhumation of coesite-bearing ultrahigh-pressure metamorphic rocks, *In:* COLEMAN R.G. & WANG X. (eds) *Ultrahigh-pressure Metamorphism*, Cambridge University Press, 159-181.

HARLEY, S.L. & CARSWELL, D.A. 1995. Ultradeep crustal metamorphism: A prospective view. *Journal of Geophysical Research*, **100**, 8367-80.

HERMANN, J., RUBATTO, D., KORSAKOV, A. & SHATSKY, V.S. 2001. Multiple zircon growth during fast exhumation of diamondiferous, deeply subducted continental crust (Kokchetav Massif, Kazakhstan). *Contribution to Mineralogy and Petrology*, **141**, 66-82.

HOLDAWAY, M.J. 1971. Stability of andalusite and the aluminium silicate phase diagram. *American Journal of Science*, **271**, 97-131.

HOLLAND, T.J.B. 1980. The reaction albite = jadeite + quartz determined experimentally in the range 600-1200°C. *American Mineralogist*, **65**, 129-134.

JAGOUTZ, E., SHATSKY, V.S. & SOBOLEV, N.V. 1990. Sr-Nd-Pb isotopic study of ultrahigh PT rocks from Kokchetav massif. EOS, Trans. AGU, *71*, 1707.

KANEKO, Y. MARUYAMA, S., TERABAYASHI, M., YAMAMOTO, H., ISHIKAWA, M., ANMA, R., PARKINSON, C.D., OTA, T., NAKAJIMA Y., KATAYAMA, I. & YAMAUCHI, K. 2000. Geology of the Kokchetav UHP-HP metamorphic belt, northern Kazakhstan. *The Island Arc*, **9**, 264-283.

KANEKO, Y., KATAYAMA, I., YAMAMOTO, H., MISAWA, K., ISHIKAWA, M., REHMAN, H.U., KAUSAR, A.B. & SHIRAISHI, K. 2003. Timing of Himalayan ultrahigh-pressure

metamorphism: sinking rate and subduction angle of the Indian continental crust beneath Asia. *Journal of Metamorphic Geology,* **21**, 589-599.

KATAYAMA, I. & NAKASHIMA, S. 2003. Hydroxyl in clinopyroxene from the deep subducted crust: Evidence for H2O transport into the mantle. *American Mineralogist*, **88**, 229-234.

KATAYAMA, I., ZAYACHKOVSKY, A. & MARUYAMA, S. 2000a. Progressive P-T records from zircon in Kokchetav UHP-HP rocks, northern Kazakhstan. *The Island Arc*, **9**, 417-428.

KATAYAMA, I., PARKINSON, C.D., OKAMOTO, K., NAKAJIMA, Y. & MARUYAMA, S. 2000b. Supersilicic clinopyroxene and silica exsolution in UHPM eclogite and pelitic gneiss from the Kokchetav massif, Kazakhstan. *American Mineralogist*, **85**, 1368-1374.

KATAYAMA, I., MARUYAMA, S., PARKINSON, C.D., TERADA, K. & SANO, Y. 2001. Ion micro-probe U-Pb zircon geochronology of peak and retrograde stages of ultrahigh-pressure metamorphic rocks from the Kokchetav massif, northern Kazkhstan. *Earth and Planetary Science Letter*, **188**, 185-198.

KATAYAMA, I., NAKASHIMA, S. & YURIMOTO, H. 2006. Water content in natural eclogite and its implication for water transport into the deep upper mantle. *Lithos*, **86**, 245-259.

KORSAKOV, A.V., SHATSKY, V.S. & SOBOLEV, N.V. 1998. First occurrence of coesite in eclogites from the Kokchetav massif, Northern Kazakhstan. *Russian Geology and Geophysics,* **34**, 40-50.

KONZETT, J., FROST, D.J., PROYER, A. & ULMER, P. 2008. The Ca-Eskola component in eclogitic cilnopyroxene as a function of pressure, temperature and bulk composition: an experimental study to 15 GPa with possible implications for the formation of oriented SiO_2-inclusions in omphacite. *Contribution to Mineralogy and Petrology*, **155**, 215-228.

KROGH, E.J. 1988. The garnet-clinopyroxene Fe-Mg geothermometer: A reinvestigation of existing experimental data. *Contribution to Mineralogy and Petrology*, **99**, 44-48.

LIATI, A. & GEBAUER, D. 1999. Constraining the prograde and retrograde P-T-t path of Eocene HP rocks by SHRIMP dating of different zircon domains: inferred rates of heating, burial, cooling and exhumation for central Rhodope, northern Greece. *Contribution to Mineralogy and Petrology*, **135**, 340-354.

LIOU, J.G., ZHANG, R.Y. & ERNST, W.G. 1994. An introduction of ultrahigh-P metamorphism. *The Island Arc*, **3**, 1-24.

LIOU, J.G., ZHANG, R.Y., ERNST, W.G., RUMBLE, D. & MARUYAMA, S. 1998. High-pressure minerals from deeply subducted metamorphic rocks. *In:* HEMLEY, R.J. (ed) *Ultrahigh-pressure Mineralogy: Physics and Chemistry of the Earth's Deep Interior*,

Mineralogical Society of America, *Review in Mineralogy*, **37**, 33-96.

LIU, F., XU, Z., LIOU, J.G., KATAYAMA, I., MASAGO, H., MARUYAMA, S. & YANG, J. 2002. Ultrahigh-P mineral inclusions in zircons from gneissic core samples of the Chinese Continental Scientific Drilling Site in eastern China. *European Journal of Mineralogy*, **14**, 499-512.

LIU, J., YE, K., MARUYAMA, S., CONG, B. & FAN, H. 2001. Mineral inclusions in zircon from gneisses in the ultrahigh-pressure zone of the Dabie Mountains, China. *Journal of Geology*, **109,** 523-535.

LUDWIG, K.R. 1991. Isoplot - a plotting and regression program for radiogenic isotope data. *In: USGS Open-File Report,* 91-445.

MAO, H.K. 1971. The system jadeite ($NaAlSi_2O_6$) - anorthite ($CaAl_2Si_2O_8$) at high pressures. *Carnegie Institute Year Book*, **69**, 163-168.

MARUYAMA, S., LIOU, J.G. & TERABAYASHI, M. 1996. Blueschists and Eclogites of the World and Their Exhumation. *International Geology Review*, **38**, 485-594.

MARUYAMA, S., TABATA, H., NUTMAN, A.P., MORIKAWA, T. & LIOU, J.G. 1998. SHRIMP U-Pb Geochronology of Ultrahigh-pressure Metamorphic Rocks of the Dabie Mountains, Central China. *Continental Dynamics*, **3**, 72-85.

MASAGO, H. 2000. Metamorphic petrology of the Barchi-Kol metabasites, western Kokchetav UHP-HP massif northern Kazakhstan. *The Island Arc*, **9**, 358-378.

MASSONNE, H.J. 2001. First find of coesite in the ultrahigh-pressure metamorphic region of the Central Erzgebirge, Germany. *European Journal of Mineralogy*, **13**, 565-570.

OGASAWARA, Y., OHTA, M., FUKASAWA, K., KATAYAMA, I. & MARUYAMA, S. 2000. Diamond-bearing and diamond-free metacarbonate rocks from Kumdy-Kol in the Kokchetav Massif, northern Kazakhstan. *The Island Arc*, **9**, 400-416.

OGASAWARA, Y., FUKASAWA, K. & MARUYAMA, S. 2002. Coesite exsolution from titanite in UHP marble from the Kokchetav Massif. *American Mineralogist*, **87**, 452-461.

OH, C.W. & LIOU, J.G. 1998. A petrogenetic grid for eclogite and related facies under high-pressure metamorphism. *The Island Arc*, **7**, 36-51.

OKAMOTO, K., LIOU, J.G. & OGASAWARA, Y. 2000. Petrological study of the diamond grade eclogite in the Kokchetav massif, northern Kazakhstan. *The Island Arc*, **9**, 379-399.

OKAMOTO, K., KATAYAMA, I., MARUYAMA, S. & LIOU, J.G. 2006. Zircon-inclusion mineralogy of a diamond-grade eclogite from the Kokchetav massif, northern Kazakhstan. *International Geology Review*, **48**, 882-891.

OTA, T., TERABAYASHI, M., PARKINSON, C.D. & MASAGO, H. 2000. Thermobaric structure of the Kokchetav UHP-HP massif deduced from a north-south traverse in the Kulet and Saldat-kol regions, northern Kazakhstan. *The Island Arc*, **9**, 328-357.

PARKINSON, C.D. 2000. Coesite inclusions and prograde compositional zonation of garnets in whiteschists of the Kokchetav Massif, Kazakhstan: a record of progressive UHP metamorphism. *Lithos*, **52**, 215-233.

PARKINSON, C.D. & KATAYAMA, I. 1999. Metamorphic microdiamond and coesite from Sulawesi, Indonesia: evidence of deep subduction as SE Sundaland Margin. *EOS, Trans. AGU,* F1181.

PARKINSON, C.D., MOTOKI, A., ONISHI, C.T. & MARUYAMA, S. 2001. Ultrahigh-pressure pyrope-kyanite granulites and associated eclogites in NeoProterozoic nappes of southeast Brazil. *In: Fluid/slab/mantle interactions and ultrahigh-P minerals: UHPM Workshop (extended abstract),* Waseda University, Tokyo, Japan, 87-90.

RUBATTO, D., GEBAUER, D. & COMPAGNONI, R. 1999. Dating of eclogite-facies zircons: the age of Alpine metamorphism in the Sesia-Lanzo Zone (Western Alps). *Earth and Planetary Science Letter*, **167**, 141-158.

RUBIE, D.C. 1986. The catalysis of mineral reactions by water and restrictions on the presence of aqueous fluid during metamorphism. *Mineralogical Magazine*, **50**, 399.

SCHERTL, H.P. & SCHREYER, W. 1996. Mineral inclusions in heavy minerals of the ultrahigh-pressure metamorphic rocks of the Dora-Maira massif and their bearing on the relative timing of the petrological events. *In:* BASU, A. & HART, S. (eds) *Earth processes: Reading the Isotopic Code*, *Geophysical Monograph,* **95**, 331-342.

SHATSKY, V.S., SOBOLEV, N.V. & VAVILOV, M.A. 1995. Diamond-bearing metamorphic rocks of the Kokchetav massif, northern Kazakhstan. *In:* COLEMAN, R. G. & WANG, X. (eds) *Ultrahigh Pressure Metamorphism,* Cambridge University Press, 427-455.

SHATSKY, V.S., JAGOUTZ, E., SOBOLEV, N.V., KOZMENKO, O.A., PARKHOMENTO, V.S. & TROESCH, M. 1999. Geochemistry and age of ultra-high pressure rocks from the Kokchetav massif, northern Kazakhstan. *Contribution to Mineralogy and Petrology*, **137**, 185-205.

SMYTH, J.R. 1980. Cation vacancies and the crystal chemistry of breakdown reactions in kimberlitic omphacites. *American Mineralogist*, **65**, 1185-1191.

SOBOLEV, N.V. & SHATSKY, V.S. 1990. Diamond inclusions in garnets from metamorphic rocks. *Nature*, **343**, 742-746.

SONG, S., YANG, J., KATAYAMA, I., LIU, F. & MARUYAMA, S. 2001. Zircons and their inclusions from various rocks in the Dulan UHP metamorphic terrane, the north Qaidam, NW China. *In: Fluid/slab/mantle interactions and ultrahigh-P minerals: UHPM Workshop (extended abstract),* Waseda University, Tokyo, Japan, 116-120.

TABATA, H., YAMAUCHI, K., MARUYAMA, S. & LIOU, J.G. 1998. Tracing the extent of a UHP metamorphic terrane: Mineral-inclusion study of zircons in gneisses from the Dabie Shan. *In:* HACKER B.R. & LIOU J.G. (eds) *When Continents Collide: Geodynamics and Geochemistry of Ultrahigh-Pressure Rocks*, Kluwer Academic Publishers, 261-73.

TERABAYASHI, M., OTA, T., YAMAMOTO, H. & KANEKO, Y. 2002. Contact metamorphism of the Daulet Suite by solid intrusion of the Kokchetav HP-UHPM slab. *In:* C.D. PARKINSON ET AL. (eds) *The Diamond-Bearing Kokchetav Massif, Kazakhstan*, Universal Academy Press, 413-426.

YE, K., YAO, Y., KATAYAMA, I., CONG, B., WANG, Q. & MARUYAMA, S. 2000. Large areal extent of ultrahigh-pressure metamorphism in the Sulu ultrahigh-pressure terrane of East China: new implications from coesite and omphacite inclusions in zircon of granitic gneiss. *Lithos*, **52**, 157-164.

ZECK, H.P. & WHITEHOUSE, M.J. 1999. Hercynian, Pan-African, Proterozoic and Archean ion-microprobe zircon ages for a Betic-Rif core complex, Alpine belt, W Mediterranean - consequences for its P-T-t path. *Contribution to Mineralogy and Petrology*, **134**, 134-149.

ZHANG, R.Y., LIOU, J.G., COLEMAN, R.G., ERNST, W.G., SOBOLEV, N.V. & SHATSKY, V.S. 1997. Metamorphic evolution of diamond-bearing and associated rocks from the Kokchetav massif, northern Kazakhstan. *Journal of Metamorphic Geology*, **15**, 479-496.

Figure captions

Fig. 1. Geological map of the Kokchetav UHP-HP massif (after Kaneko *et al.* 2000).

Fig. 2. Photomicrographs (plane polarized light) showing diamond inclusions (a, b, c, d, e, f) and coesite inclusions (g, h, i) in zircon from the Kokchetav UHP metamorphic rocks. (f): sketches of graphite and diamond aggregates in zircon.

Fig. 3. Representative Raman spectra of (a) diamond and (b) coesite. Inclusion spectra always contain host zircon peaks at 359-362 cm^{-1}, 440-445 cm^{-1} and 1010-1013 cm^{-1}.

Fig. 4. (a) Inclusions in zircon from metapelites. (b) Host minerals in metapelites. Metamorphic zones and units are modified after Ota *et al.* (2000).

Fig. 5. Photomicrographs of matrix and inclusion minerals of the Kokchetav UHP rocks. (a)

Omphacite of eclogite contains abundant quartz rods. (b) Diopside from diamond-bearing marble contains exsolved lamellae of phengite. (c), (d) Omphacite inclusion in zircon from eclogite. Quartz rods are absent in the inclusion. (e) Diopside inclusion in zircon from marble, which is in contact with microdiamond inclusion.

Fig. 6. Clinopyroxene compositions plotted on Augite(Aug)-Jadeite(Jd)-Ca-Eskola(CaEs) diagram (modified after Katayama *et al.* 2000b).

Fig. 7. Garnet compositions of inclusion and matrix plotted on ternary diagram of (Almandin+Spessartin)-Grossular-Pyrope. (a) Coesite-bearing eclogite, and (b) diamond-bearing biotite gneiss.

Fig. 8. Composition of analyzed inclusion and matrix phengites from pelitic gneisses. Inclusions show higher Si content than those in the matrix of the rocks, whereas Fe/(Fe+Mg) ratio of the inclusion and matrix phengites are relatively limited in the each samples.

Fig. 9. Cathodoluminescence images of zircons from diamond-bearing gneiss (a,b) and back-scattered electron images of zircons from low-grade schist (c) and from eclogite (d). Zircon from eclogite has no zonal texture and contains numerous inclusions including omphacite, garnet and coesite, whereas zircon from gneiss and schist show clear zonal texture with distinct inclusion micro-assemblages.

Fig. 10. Mineral inclusion assemblage in the different zircon domains of diamond-bearing gneisses.

Fig. 11. Tera-Wasserburg diagram of SHRIMP analyses of the different zircon domains of the diamond-bearing gneisses and low-grade schist (modified after Katayama *et al.* 2001).

Fig. 12. Histogram of apparent $^{206}Pb/^{238}U$ age of the different zircon domains of each lithologies. The different zircon domains show apparently different ages.

Fig. 13. REE patterns of zircon from diamond-bearing gneisses (a,b), eclogite (c), and low-grade schist (d). REE patterns are normalized to chondrite (Anders & Grevesse 1989).

Fig. 14. Generalized *P-T*-time path for UHP-HP metamorphic rocks from the Kokchetav massif with geotherms (5°C/km and 20°C/km). The *P-T* estimates are derived from this study (black field) and previous studies (Shatsky *et al.* 1995; Zhang *et al.* 1997; Okamoto *et al.* 2000; Ogasawara *et al.* 2000; Terabayashi *et al.* 2002). SHRIMP analysis of different zircon domains distinguished the metamorphic history of the

Kokchetav UHP-HP rocks into four different stages: 1100-1400 Ma protolith age (stage 1), 537 ± 9 Ma for the UHP metamorphic origin (stage 2), 507 ± 9 Ma for the retrograde overprinting origin (stage 3), 456-460 Ma for late granitoid intrusion origin (stage 4). Petrogenetic grids, subdivision of eclogite facies, stability fields of Al_2SiO_5 polymorphs, and reaction curves; diamond = graphite, coesite = quartz and jadeite + quartz = albite are from Oh & Liou (1998), Holdaway (1971), Bundy (1980), Bohlen & Boettcher (1982) and Holland (1980).

Table 1. Representative mineral inclusion assemblages in zircon from the Kokchetav UHP-HP massif.

locality	sample no.	rock type	Dia	Grp	Coe	Qtz	Grt	Phe	Phl	Rt	Ab	Kfs	Amp	Cpx	Zo	Ky	Cal	Dol	Ap	Mz
Barchikol	F464	pelitic gneiss				+	+	+		+										
Barchikol	F466	pelitic gneiss		+		+	+	+		+	+									
Barchikol	F469	amphibolite				+	+			+		+	+	+						
Barchikol	H318	ortho gneiss				+		+	+		+	+							+	+
Barchikol	K361	quartzite			+	+							+	+			+	+		
Barchikol	K364	eclogite				+	+			+		+		+	+				+	
Barchikol	Y410	quartzite		+		+		+									+		+	
Kumdykol	A8	pelitic gneiss	+	+	+	+	+			+				+					+	
Kumdykol	A12	pelitic gneiss	+	+	+	+		+								+				
Kumdykol	A28	pelitic gneiss		+		+	+	+		+	+									
Kumdykol	A30	pelitic gneiss		+		+	+	+		+									+	
Kumdykol	A21	eclogite			+	+	+			+	+		+	+					+	
Kumdykol	A60	eclogite			+	+	+			+				+					+	
Kumdykol	H2	pelitic gneiss	+		+		+										+			
Kumdykol	H5	pelitic gneiss	+	+													+			
Kumdykol	K18	pelitic gneiss		+		+		+				+							+	
Kumdykol	K183	eclogite					+			+	+	+	+	+	+				+	
Kumdykol	N21	meta carbonate	+	+	+		+						+	+			+	+	+	
Kumdykol	N57	eclogite				+	+			+			+	+						
Kumdykol	XX7	ortho gneiss		+		+		+											+	
Chaglinka	K145	pelitic gneiss		+		+	+	+											+	
Chaglinka	M121	pelitic gneiss		+		+		+		+									+	
Chaglinka	T63	pelitic gneiss				+		+		+										
Kulet	F256	pelitic gneiss		+		+		+												
Kulet	F265	pelitic gneiss				+		+		+		+							+	
Kulet	T264	pelitic gneiss		+		+		+											+	
Sulu-Tjube	F44	pelitic gneiss				+		+	+			+							+	
Sulu-Tjube	N81	pelitic schist				+						+							+	
Soldatkol	F375	quartz schist		+		+													+	+
Unit I	A157	pelitic schist				+														
Unit III	Y276	ortho gneiss		+		+		+											+	

Mineral abbreviations: Dia, diamond; Grp, graphite; Coe, coesite; Qtz, quartz; Phe, phengite;Phl, phlogopite; Rt, rutile; Ab, albite; Kfs, K-feldspar Amp, amphibole; Cpx, clinopyroxene; Zo, zoisite; Ky, kyanite; Cal, calcite; Dol, dolomite; Ap, apatite; Mz, monazite

Table 2. Isotopic ages of the Kokchetav UHP-HP rocks

isotopic method	protolith age	UHP peak age	retrograde age	ref.
U-Pb zircon assisted by inclusion	1300-1100 Ma	537±9 Ma	507±8 Ma	1
U-Pb zircon (average)	ca. 2000 Ma	530±7 Ma		2
Sm-Nd of garnet and omphacite	ca. 2200 Ma	533±20 Ma		3
Pb-Pb of whole rock	ca. 1500 Ma			4
Ar-Ar of muscovite			517±5 Ma	4
Ar-Ar of biotite			516±5 Ma	4

References; 1: Katayama *et al*. (2001), 2: Claoue-Long *et al*. (1991), 3: Jagoutz *et al*. (1990), 4: Shatsky et al. (1999).

Table 3. P-T estimate of various rock types in the Kokchetav UHP rocks

rock type	locality	prograde stage	peak stage	retrograde stage	ref.
Eclogite	Kumdykol		970-1110°C, 60-80 kbar	840°C, P<15 kbar	1
Grt-Bt gneiss	Kumdykol		950-1100°C, P>40 kbar	740-790°C, P~10 kbar	1
Dolomitic marble	Kumdykol	T<850°C, P>28 kbar	980-1020°C, 60-70 kbar		1
Eclogite	Kumdykol		840-1000°C, P>40 kbar		2
Eclogite	Kumdykol		785°C, P>30 kbar	680°C, ca.10 kbar	3
Eclogite	Kumdykol		1000°C, 60 kbar	750-950°C, ca. 10 kbar	5
Grt-Bt gneiss	Kumdykol		800-920°C, P>40 kbar		2
White schist	Kulet	430-580°C, 8-19 kbar	750-800°C, P>28 kbar		3
Pyroxene-carbonate rock	Kumdykol		1120°C, P>40 kbar		2
Dolomitic marble	Kumdykol		900-1000°C, P>40 kbar	790°C	3
Dolomitic marble	Kumdykol		980-1250°C, 40-70 kbar	800-950°C, 15 kbar	4

Reference; 1: This study, 2: Shatsky *et al*. (1995), 3: Zhang *et al*. (1997), 4: Ogasawara *et al*. (2000), 5: Okamoto *et al*. (2000)

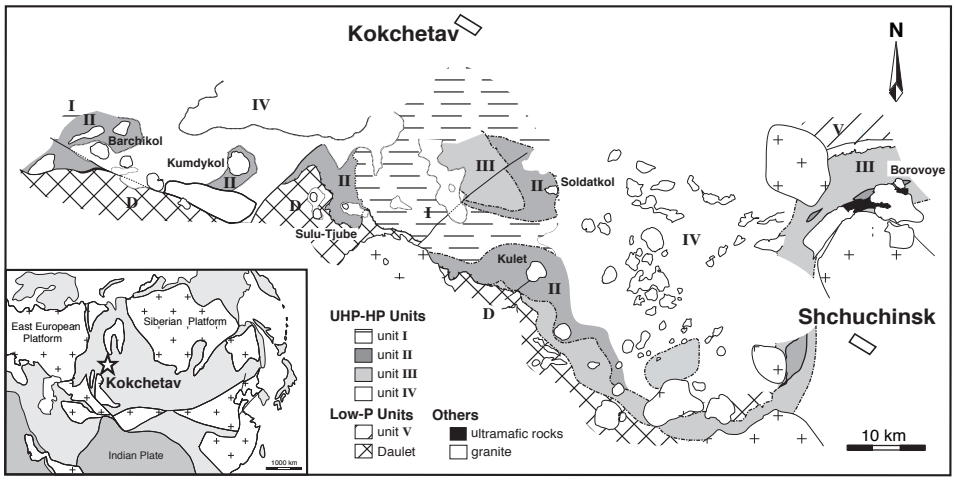

Fig 1. Katayama and Maruyama

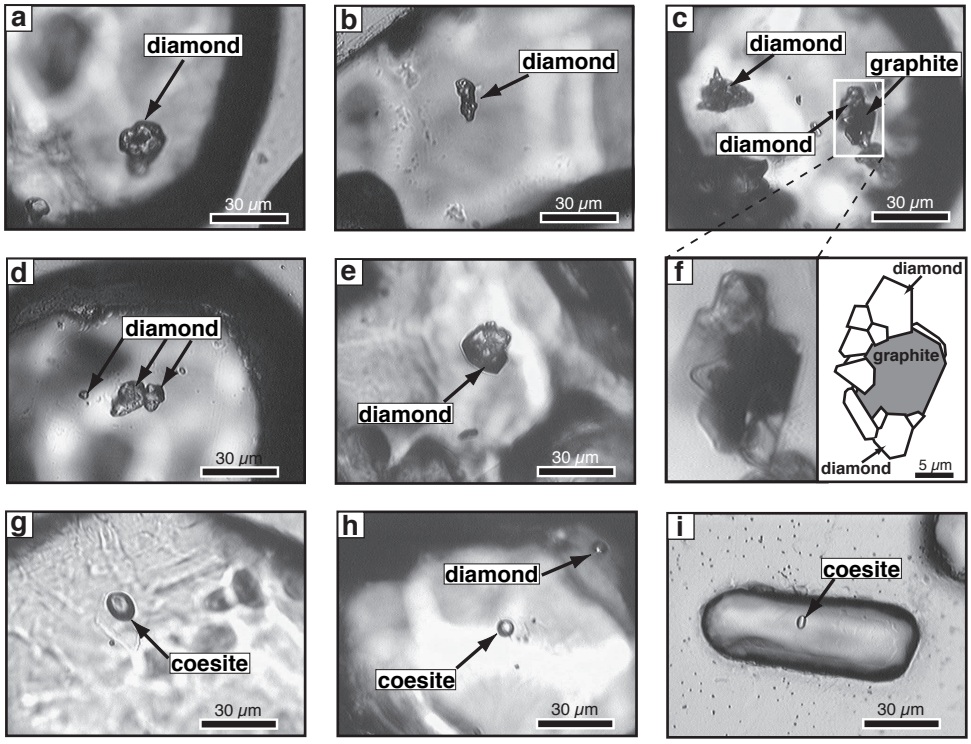

Fig. 2. Katayama and Maruyama

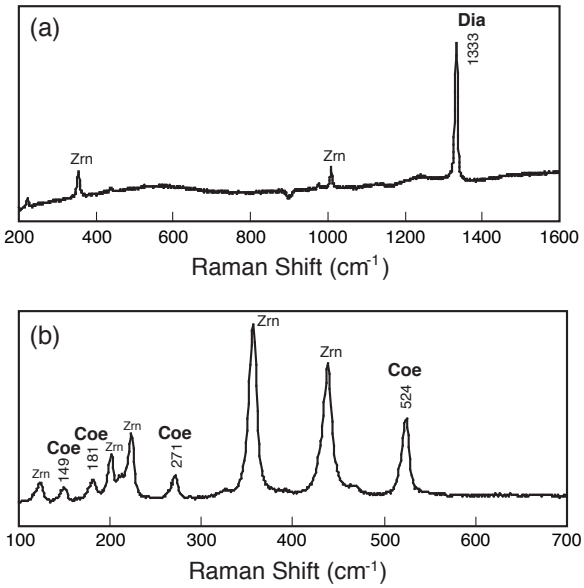

Fig. 3. Katayama and Maruyama

(a) Mineral inclusion in zircon

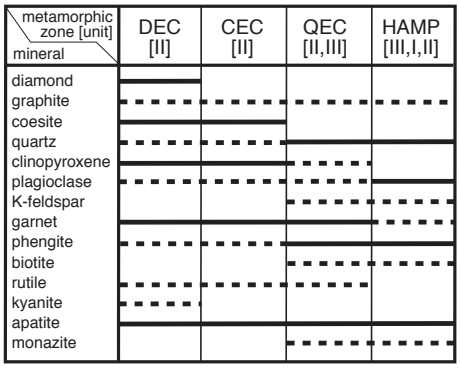

(b) Host metapelite

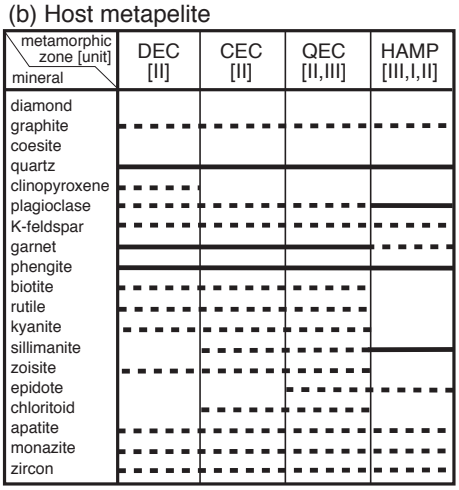

DEC: diamond-eclogite zone, CEC: coesite-eclogite zone,
QEC: quartz-eclogite zone, HAMP: high-pressure amphibolite zone

common rare

Fig. 4. Katayama and Maruyama

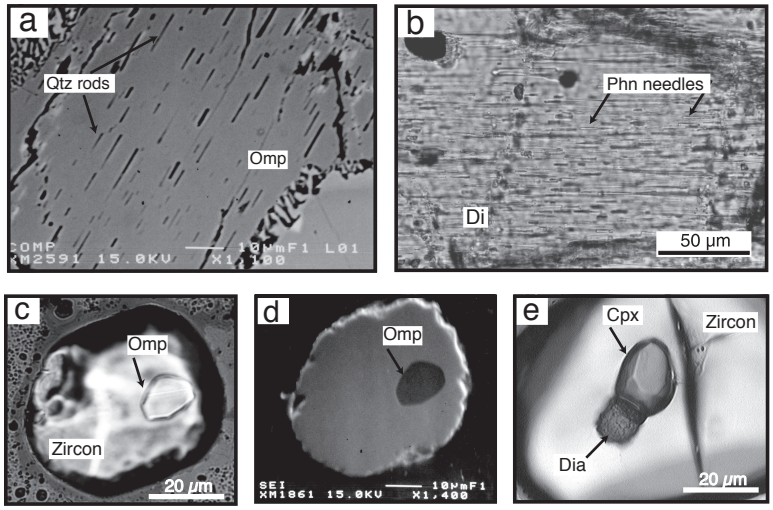

Fig. 5. Katayama and Maruyama

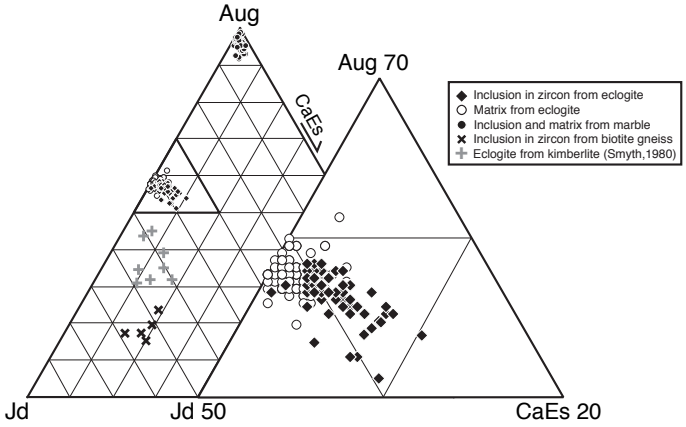

Fig. 6. Katayama and Maruyama

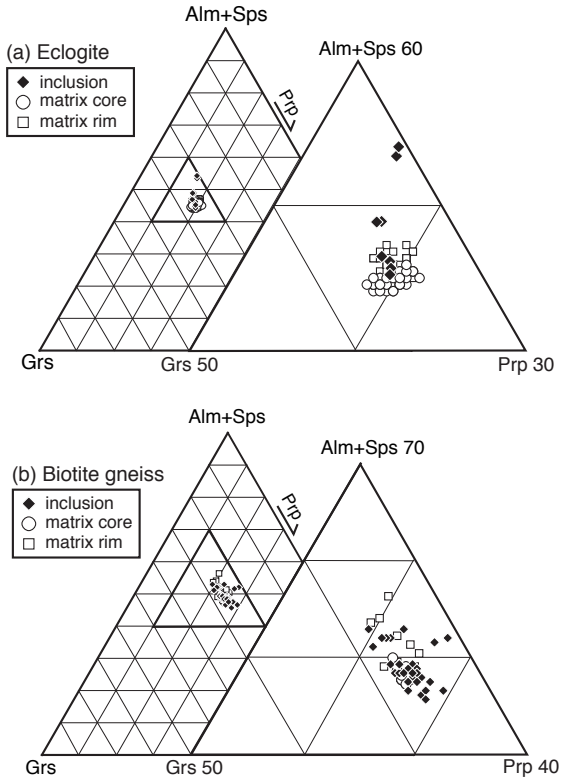

Fig. 7. Katayama and Maruyama

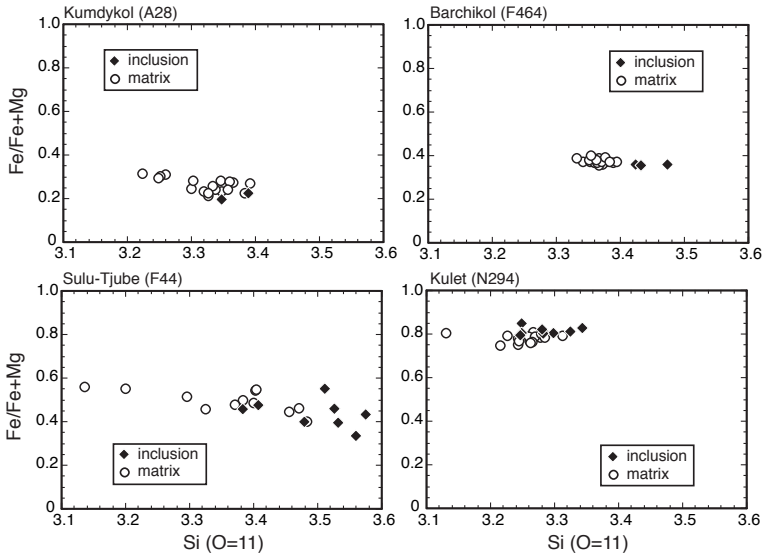

Fig. 8. Katayama and Maruyama

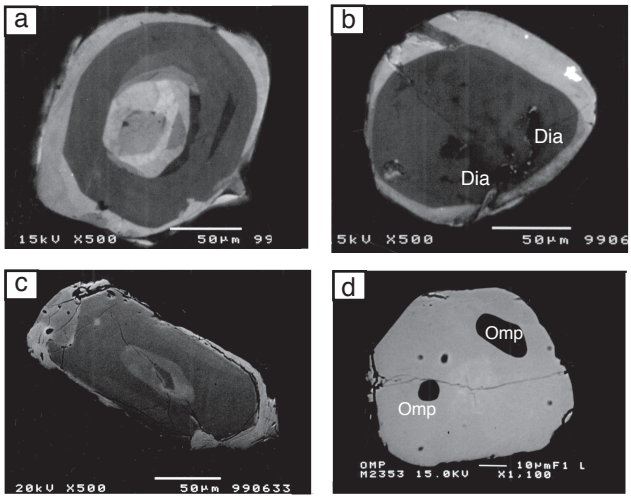

Fig.9. Katayama and Maruyama

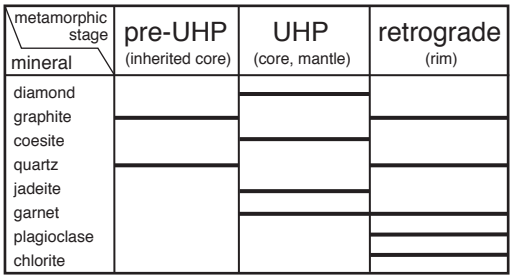

Fig. 10. Katayama and Maruyama

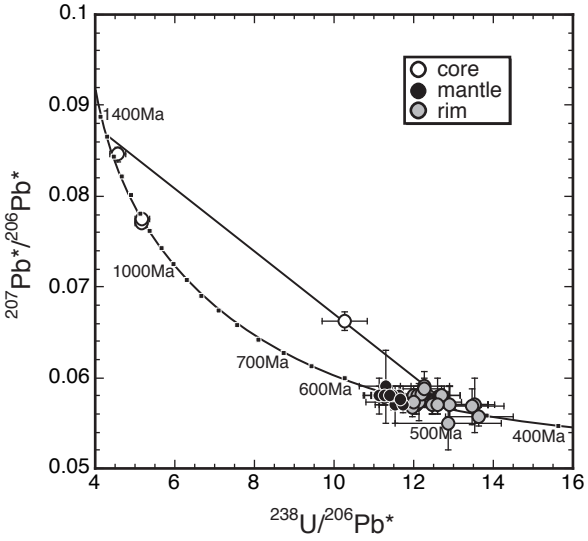

Fig. 11. Katayama and Maruyama

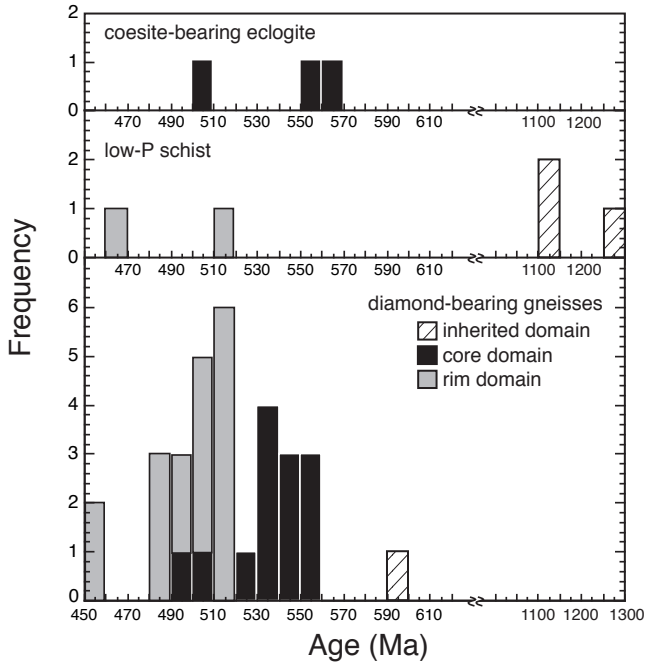

Fig. 12. Katayama and Maruyama

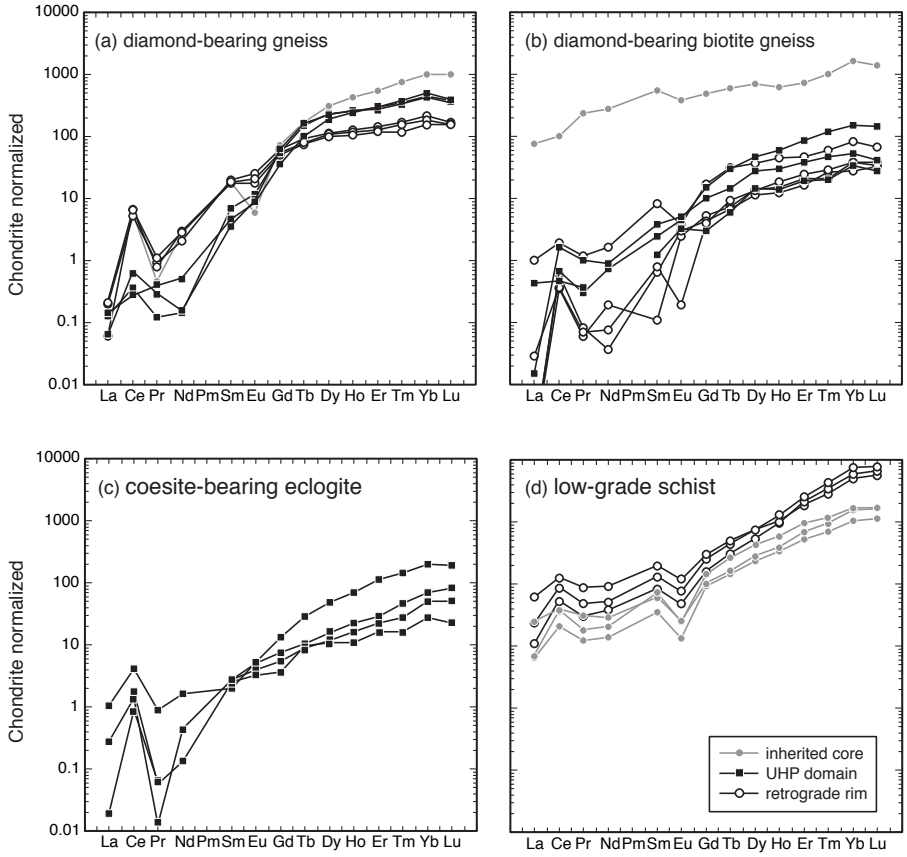

Fig. 13. Katayama and Maruyama

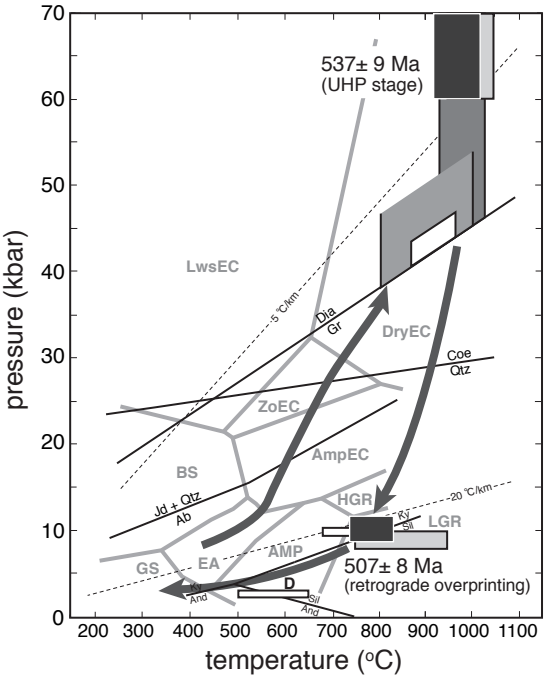

Fig. 14. Katayama and Maruyama